




ORIGINAL RESEARCH

Understanding wind turbine power converter reliability under realistic wind conditions

 Sermed Alsaadi  | Christopher J. Crabtree  | Peter C. Matthews | Mahmoud Shahbazi 

 Department of Engineering, Durham University,
Durham, United Kingdom of Great Britain and
Northern Ireland

Correspondence

 S. Alsaadi, Department of Engineering, Durham
University, Durham, United Kingdom of Great
Britain and Northern Ireland.
Email: sermed.a.alsaadi@durham.ac.uk

Funding information

 UKRI EPSRC Prosperity Partnership in Offshore
Wind, Grant/Award Number: EP/R0049/1

Abstract

The reliability of wind turbine power converters is crucial for analyzing wind energy project costs, and for estimating maintenance and downtime. The published literature in this field relies on evaluating the reliability effect of wind speed to estimate the converter lifetime. However, this paper demonstrates that wind turbulence intensity, which has not been widely considered in similar reliability analyses, shows a significant impact on converter lifetime. This paper uses 821 10-min wind speed time series sampled at 1 Hz on the two most commonly deployed wind turbine converter topologies: the two-level voltage source and the three-level neutral point clamped. Electromechanical and thermal modelling, combined with statistical analysis shows that mean wind speed and turbulence intensity both impact the lifetime of both converter topologies. However, the paper estimates that the three-level converter can operate 2.4 to 4.0 times longer than the two-level converter depending on the operating wind speed and turbulence intensity.

1 | INTRODUCTION

Wind turbine (WT) reliability impacts the cost of wind energy due to WT downtime and the cost of maintenance [1]. The reliability data of WT subassemblies show that the wind turbine power converter (WTPC) ranks as one of the highest failing parts in the system [2]. WTPC reliability analysis provides the device's end-of-life estimation which is important information required for the cost analysis of the new wind farms and the maintenance planning of the operational farms.

After frequent and costly failures of WTPC, a large group of researchers from academia and industry joined the investigations of the impacting factors and causes of failures [3]. The semiconductor thermal loading was found to be the main cause of failure in WTPC [4]. The differences in the thermal expansion coefficient of the semiconductor internal parts and the cycling junction temperature develop a cyclic thermomechanical stress that causes damage in the semiconductor [5]. Methods for estimating converter lifetime based on its semiconductor's thermal cycling are widely used by academia [6–8] and industry [9, 10]. Empirical lifetime models like Coffin–Manson Arrhenius [5] and Bayerer [11] estimate semiconductor lifetime based on junction temperature cycling.

Current state-of-the-art WTs have adopted the permanent magnet synchronous generator (PMSG). This generator type requires a full power back-to-back AC–DC–AC converter for energy conversion and control. Two converter topologies have been used with PMSG WTs: the two-level voltage-source converter (2L-VSC) and the three-level neutral point clamped converter (3L-NPC). The 3L-NPC provides higher operating voltage with reduced current which reduces the size of cables and transformer. However, it requires more semiconductors than 2L-VSC and needs more complex control and maintenance. 3L-NPC is the preferred topology with medium voltage (MV) applications like MV wind turbines while 2L-VSC is preferred with low voltage (LV) applications. Examples of LV WTs equipped with 2L-VSC include Siemens Gamesa SWT-7.0/SG-8.0, MHI Vestas V164-8.0 and Enercon E126-7.58 [3]. While MV WTs equipped with 3L-NPC include GE Haliade-X [12] and Samsung S7.0.171 [13]. The published literature in this field focuses on the relationship between the operating wind speed and the reliability of WTPC where the reliability analyses show wind speed has a direct impact on the lifetime of the converter's semiconductors. The relationship between wind speed and WTPC reliability is widely discussed [6, 7, 14, 15].

This is an open access article under the terms of the [Creative Commons Attribution](https://creativecommons.org/licenses/by/4.0/) License, which permits use, distribution and reproduction in any medium, provided the original work is properly cited.

© 2024 The Authors. *IET Power Electronics* published by John Wiley & Sons Ltd on behalf of The Institution of Engineering and Technology.

Besides the average wind speed, WTPC reliability is also impacted by other wind parameters like gust frequency and turbulence intensity [14, 16]. Wind turbulence intensity (TI) is an important parameter that can be extracted from the wind speed data. The TI of a wind speed time series (WSTS) is expressed as the percentage value of the standard deviation of wind speed measurements (U_σ) divided by the WSTS average wind speed (U_{avg}) [17], as in Equation (1).

$$TI = \frac{U_\sigma}{U_{avg}} \cdot 100\% \quad (1)$$

A few published articles introduced the possibility of a relationship between TI and WTPC reliability. In [14], the impact of wind gust frequency on the semiconductors' lifetime in WTPC has been presented. The paper analyzed the impact of wind gust frequency on the reliability of the 2L-VSC WTPC by simulating the thermal loading of the converter semiconductors. The results showed that thermal loading increases at slower wind gust frequency. Accordingly, the paper concluded that lower turbulence sites would have a more damaging impact on the WTPC. The paper built that conclusion based on the results of simulations using synthetic constant and square wave wind speed time series. However, a simulation with field-measured wind speed data would have provided more realistic results of the impact of wind turbulence on WTPC lifetime.

In [7], The reliability interactions between wind roughness classes and the WTPC modulation method have been presented. The paper tested the lifetime of 3L-NPC WTPC using thermal loading simulation with different wind roughness classes. Based on the simulation results, the paper suggested that a certain type of converter pulse width modulation (PWM) achieves better converter reliability during high roughness class wind. Accordingly, the paper concluded that higher turbulence intensity wind has a negative reliability impact on the WTPC. However, the paper did not analyze nor evaluate the mentioned impact. This paper's conclusion conflicts with the findings of the previous paper.

In [18], the thermal loading of the WTPC semiconductors is assessed against the wind speed dynamics. The paper simulated the WTPC semiconductor junction temperature of a 1.5 MW WT while applying a 180 WSTS. The visual comparison between the WTPC semiconductors' simulated junction temperature and the wind speed trends showed that during the high-frequency wind speed changes, the semiconductors had lower thermal loading. The paper found that it is reasonable to assume that low-frequency turbulence winds produce a higher damage rate to the WTPC. However, the paper's conclusion was based on the results of only one 180-s WTST without demonstrating further analysis to evaluate the results.

The reviewed papers as well as other published papers on this subject assess WTPC reliability either based on constant wind speeds, synthetic wind samples, or a small number of WSTS. The practical loading of the WT is complex due to the nature

of wind and, as such, is the WTPC reliability assessment. Therefore, WTPC reliability analysis has to consider a wide range of wind speeds and use statistical analysis to approach the expected lifetime. Furthermore, statistical analysis would be the best way to determine the impact of wind TI on WTPC lifetime since TI is a statistically calculated value based on the standard deviation of wind speed as in Equation (1).

This paper analyzes that relationship by applying field-measured wind speed data on the two most commonly deployed WTPC topologies in WTs, 2L-VSC and 3L-NPC. The paper uses the WTPC's semiconductor thermal loading to assess the WTPC lifetime and analyze the effects of wind conditions. Furthermore, the paper demonstrates the reliability comparison between both WTPC topologies for the same input wind to identify which converter shows better reliability for the particular tested wind characteristics.

2 | WTPC MODELLING AND RELIABILITY ANALYSIS

The reliability of a WTPC is highly influenced by the lifetime of its semiconductors where the thermal cycling of their junction temperature is considered the main cause of WTPC failure [8]. The semiconductor lifetime can be estimated by the Coffin–Manson Arrhenius model. This considers the range and average of their junction temperature cycles to calculate the accumulated damage and accordingly the estimated lifetime. Semiconductor junction temperature is a function of the semiconductor power losses which depend on the WTPC loading and thus the wind speed. The semiconductor junction temperature affects its internal parameters which impact its junction temperature in an iterating process. Junction temperature estimation of WTPC semiconductors during variable wind speed is complex and therefore system simulation is chosen to provide a suitable approach.

The two most widely deployed converters in WTs (2L-VSC and 3L-NPC) are modelled in two separate models for reliability analysis. Both models involve mechanical, electrical, and thermal subsystems to capture the system dynamics in the simulation results. Both models are based on 2 MW PMSG direct-drive variable-speed wind turbines. The overview of the wind turbine model is shown in Figure 1 where ω_m is the WT generator speed (rad/s), T_{ref} is the reference torque (Nm), I_m is the generator current (Ampere), FOC is the field-oriented control, and SVPWM is the space vector pulse width modulation. The shaded blocks in the diagram represent the reliability-related subsystems showing the corresponding sections of this section while the other blocks are modelled as required for the WT operation and control. The WT parameters and control design are based on [19] and shown in Table 1. MATLAB and Simulink are used in the modelling and simulating of both WT models, 2L-VSC and 3L-NPC. The following sections describe the modelling of the reliability-related subsystems as indicated in Figure 1.

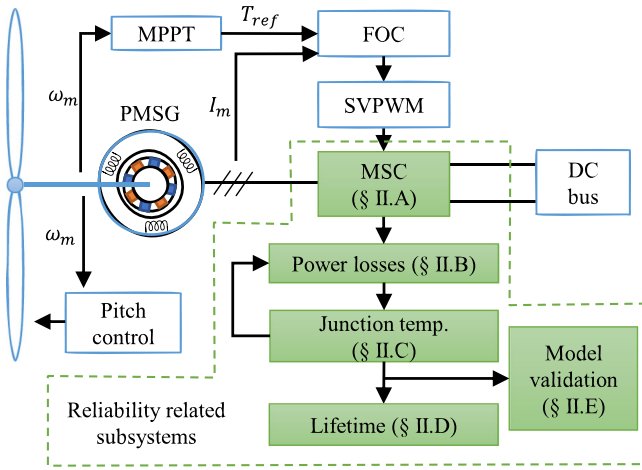


FIGURE 1 Wind turbine model overview.

TABLE 1 Wind turbine parameters.

Wind turbine type	Direct-drive variable speed
Cut-in wind speed (m/s)	4
Rated wind speed (m/s)	12
Cut-out wind speed (m/s)	25
Rotor diameter (m)	82
Power coefficient, $C_{p_{max}}$	0.34
Rotor moment of inertia (kg m ²)	2,920,000
Generator type	Three-phase PMSG
Generator rated power (kW)	2,000
Generator rated apparent power (kVA)	2,242
Generator number of pole pairs	26
Generator rated frequency (Hz)	9.75

2.1 | Converter system

A PMSG WT usually employs a fully rated power AC–DC–AC converter which consists of a machine-side converter (MSC) and a grid-side converter (GSC). The MSC is connected between the generator and the DC bus and is responsible for extracting the generator power. The GSC is connected between the DC bus and the grid transformer and is responsible for providing regulated DC voltage in the DC bus. The GSC shows a lower failure rate (higher lifetime) than the MSC because it operates at fixed grid frequency and voltage. Therefore, the WTPC system reliability is dominated by the MSC [14, 20]. The MSC lifetime is considered for the WTPC reliability analysis in this paper while the GSC is substituted with a DC supply to reduce model complexity and simulation time.

The two WT models, 2L-VSC and 3L-NPC, have the same WT mechanical subsystem and the same control and use the same input of WSTS for reliability analysis and comparison. However, they vary by the operating voltage as 3L-NPC is usu-

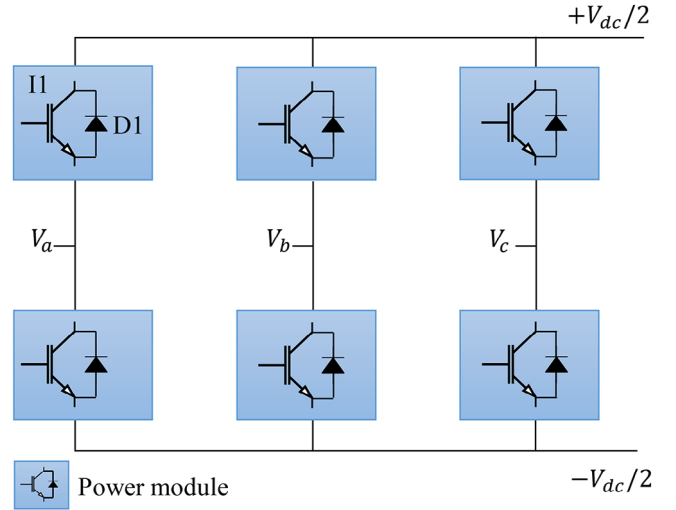


FIGURE 2 Schematic diagram of three-phase 2L-VSC.

ally deployed in MV WTs (rated generator voltage is above 1 kV) while 2L-VSC is deployed in LV WTs, (rated generator voltage is below 1 kV). The following paragraphs describe the modelling of both converters.

2.1.1 | 2L-VSC

This converter model is constructed with six power modules each having an IGBT and a reverse parallel diode. Semikron's power module SKM800AG167D [21] is selected for this model due to its ratings and the specified application area by the manufacturer. Accordingly, the modelled converter's rated power is 335 kW. Therefore, six converters are required to operate in parallel to handle the generator's rated power (2 MW). Parallel converters are used in WTs to share the generator power. An example of this is the Siemens G10x 4.5 MW where six converters are placed in parallel [22]. The converter subsystem schematic diagram is shown in Figure 2 where I1 is IGBT1, D1 is diode1, $V_{a,b,c}$ are the AC three-phase voltages.

2.1.2 | 3L-NPC

This converter model is assembled with 18 power modules as shown in the schematic diagram in Figure 3. Similar to the 2L-VSC power module, SKM800AG167D is selected for the 3L-NPC model for the reliability comparison. The 3L-NPC operating voltage is twice the power module's rated voltage [4]. Therefore, the 3L-NPC rated voltage is twice the 2L-VSC rated voltage when both converters are constructed using the same power module. However, both converters will have the same current capacity which is equal to the power module's rated current and that makes the modelled 3L-NPC rated power 670 kW. Accordingly, only three parallel 3L-NPC are required to handle the generator's rated power (2 MW). The parameters of the 2L-VSC and 3L-NPC models are listed in Table 2.

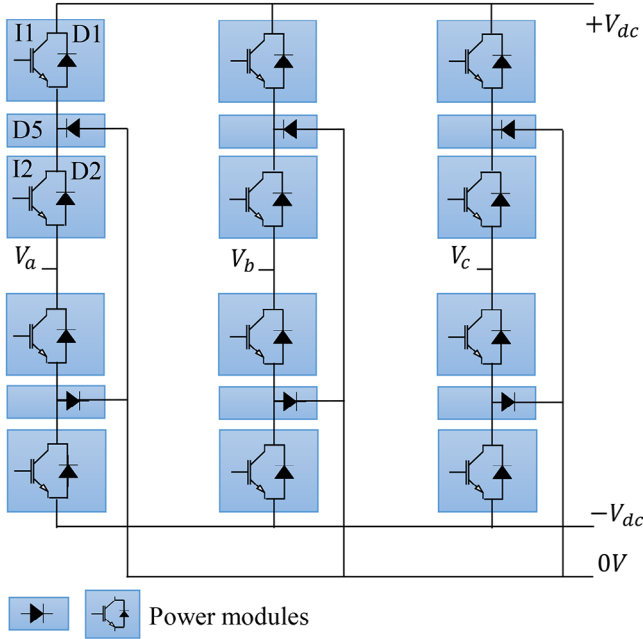


FIGURE 3 Schematic diagram of three-phase 3L-NPC.

TABLE 2 2L-VSC and 3L-NPC models parameters.

Converter topology	2L-VSC	3L-NPC
Rated power of one converter (kW)	335	670
Number of parallel converters in WT	6	3
Total rated power (kW)	2,000	2,000
Total number of IGBTs	36	36
Total number of diodes	36	54
DC bus voltage (V)	1150	2300
Generator line voltage (V)	230-690	460-1380
Power module	SKM800AG176D	
Heatsink cooling method	Liquid	
Coolant temperature (C)	40	
Generator frequency (Hz)	3.25-9.75	
Control strategy	FOC	
Switching frequency (Hz)	1900	

2.2 | Power losses

The converter semiconductors' lifetime is highly impacted by their junction temperature which varies as a function of their power losses and the heatsink thermal characteristics. Semiconductors' power loss modelling is essential in WTPC reliability analysis. Two types of power losses are produced by the semiconductor when operating as a switch as in a WTPC: the switching power losses (P_{sw}) and the conduction power losses (P_{cn}). The switching power losses occur when the semiconductor changes its status between on and off states while the conduction power loss develops when the semiconductor is on. Equations (2) to (4) describe the IGBT conduction, switching,

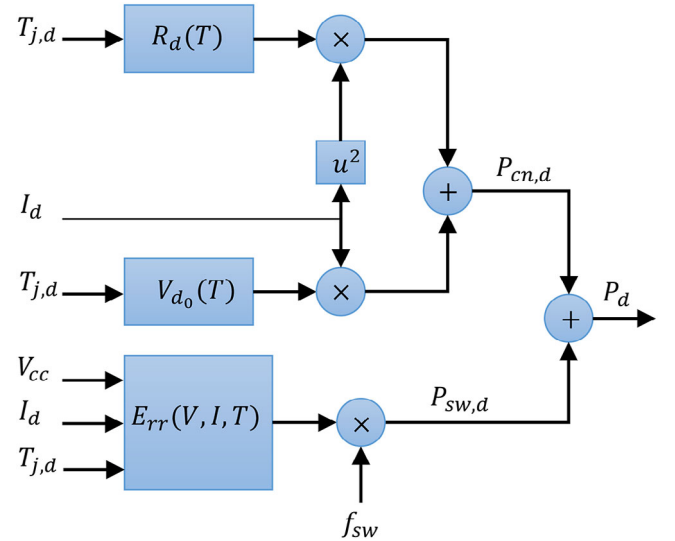


FIGURE 4 Diode power losses in power converter.

and total power losses respectively where V_{ce0} is the collector-emitter threshold voltage, I_c is the IGBT current, R_{ce} is the IGBT conduction resistance, V_{cc} is semiconductor operating voltage, $P_{cn,i}$ is the IGBT conduction power loss, f_{sw} is converter switching frequency, E_{on} and E_{off} are the IGBT on and off energy, $P_{sw,i}$ is the IGBT switching power loss, and P_i is the IGBT power losses. Similarly, the diode power losses (P_d) are calculated based on the diode parameters.

$$P_{cn,i} = V_{ce0} \cdot I_c + R_{ce} \cdot I_c^2 \quad (2)$$

$$P_{sw,i} = f_{sw} \cdot (E_{on} + E_{off}) \quad (3)$$

$$P_i = P_{cn,i} + P_{sw,i} \quad (4)$$

The semiconductor's internal parameters are affected by temperature, voltage, and current according to the manufacturer datasheet [21]. Therefore, their values are required to be updated with the related affecting parameters during the simulation. Figure 4 shows the modelling of the diode power losses where $P_{cn,d}$ and $P_{sw,d}$ are the conduction and switching power losses, $T_{j,d}$ is the diode junction temperature, I_d is the diode current, E_{rr} is the reverse recovery energy, V_{d0} is the threshold voltage, and R_d is the diode on status internal resistance. Similarly, the IGBT power losses are modelled.

2.3 | Thermal modelling

It is difficult to measure the semiconductor's junction temperature and it is complex to calculate it during the variable load of the WTPC. Therefore, thermal modelling is used to determine it in this paper by using the thermal equivalent circuit. The semiconductor power loss is modelled as a current source and the junction temperature is the measured voltage. The thermal impedance, (Z_{th}), includes thermal resistance, (R_{th}), and thermal

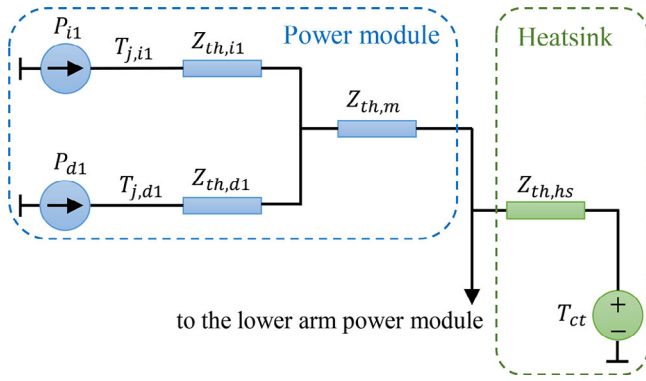


FIGURE 5 Thermal equivalent circuit of the half-bridge upper arm in 2L-VSC.

storage, (C_{th}) , are obtained from the semiconductor datasheet and the heatsink parameters. The thermal equivalent circuit is modelled using the Foster model as it is widely used in similar analyses [7]. MATLAB Simscape Thermal Model toolbox [23] components are used in modelling the converter equivalent thermal circuit.

Assuming normal WT operation conditions, the converter phases are balanced and the converter upper arm and lower arm in each half-bridge are operating symmetrically, then only one arm of each converter topology is needed to be modelled. The thermal equivalent circuit of the 2L-VSC half-bridge upper arm with the attached heatsink is shown in Figure 5 while the 3L-NPC half-bridge upper arm with the attached heatsink is shown in Figure 6 where $Z_{th,i}$ and $Z_{th,d}$ are the IGBT and the diode thermal impedances, $Z_{th,m}$ is the thermal impedance of the power electronic module, $Z_{th,hs}$ is the thermal impedance of the heatsink, $T_{j,i}$ and $T_{j,d}$ are the IGBT and diode junction temperatures, and T_{ct} is the heatsink coolant temperature.

2.4 | WTPC lifetime

The WTPC lifetime is estimated based on the lifetimes of its semiconductors, IGBTs and diodes, where the Coffin–Manson Arrhenius lifetime model [5] is used for that as recommended by the power module manufacturer [9]. The lifetime model estimates the number of thermal cycles that the semiconductor can withstand before it will fail which is known as the cycles to failure (N_f) calculated for each thermal cycle as a function of the average and range of the junction temperature as in Equation (5) where T_m is the semiconductor average junction temperature, ΔT is the junction temperature cyclic range, K_B is the Boltzmann constant (1.381×10^{-23} J/K), E_g is the semiconductor activation energy (9.891×10^{-20} J), a and b are the model empirical constants, (2.025×10^5) and (5.039) respectively as they set by the semiconductor manufacturer data [9]. The WT model simulation provides the time trend of WTPC semiconductor junction temperature related to the WSTS input. The Rainflow algorithm [5] is used to extract the thermal cycles where each one contributes an amount of damage (D_f) to the semiconductor calculated by Equation (6). According to Miner’s rule [24],

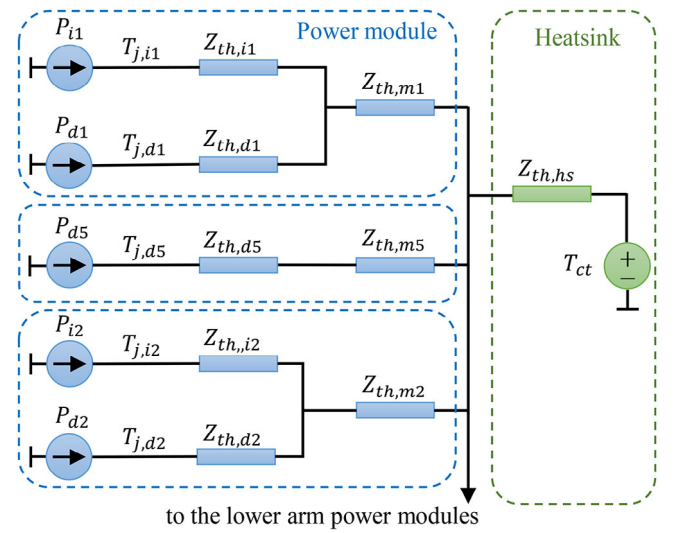


FIGURE 6 Thermal equivalent circuit of the half-bridge upper arm in 3L-NPC.

the semiconductor accumulated damage (D_{ws}) that occurred during the WSTS time (t_{ws}) is the sum of damages of all thermal cycles of that time calculated as in Equation (7).

$$N_f = a \cdot (\Delta T)^{-b} \cdot e^{E_g / (K_B T_m)} \quad (5)$$

$$D_f = \frac{1}{N_f} \quad (6)$$

$$D_{ws} = \sum_{t=0}^{t=t_{ws}} D_f(t) \quad (7)$$

Mean time to failure (MTTF) in hours is used to evaluate the lifetimes of the WTPC based on its IGBTs and diodes lifetime. The IGBT lifetime ($MTTF_i$) related to the tested WSTS is calculated as in Equation (8) where $D_{ws,i}$ is the IGBT accumulated damage and the diode lifetime ($MTTF_d$) is calculated as in Equation (9) where $D_{ws,d}$ is the diode accumulated damage. The WTPC is considered a system of stressed parts, IGBTs and diodes, where its rate of failure equals the sum of the parts rates of failure. The WTPC’s lifetime ($MTTF_{pc}$) is calculated considering the lifetime of all the IGBTs and diodes in the converter circuit as in Equation (10) where s_i and s_d are the numbers of IGBTs and diodes in the converter circuit respectively.

$$MTTF_i = \frac{t_{ws}}{D_{ws,i}} \quad (8)$$

$$MTTF_d = \frac{t_{ws}}{D_{ws,d}} \quad (9)$$

$$MTTF_{pc} = \left(\frac{s_i}{MTTF_i} + \frac{s_d}{MTTF_d} \right)^{-1} \quad (10)$$

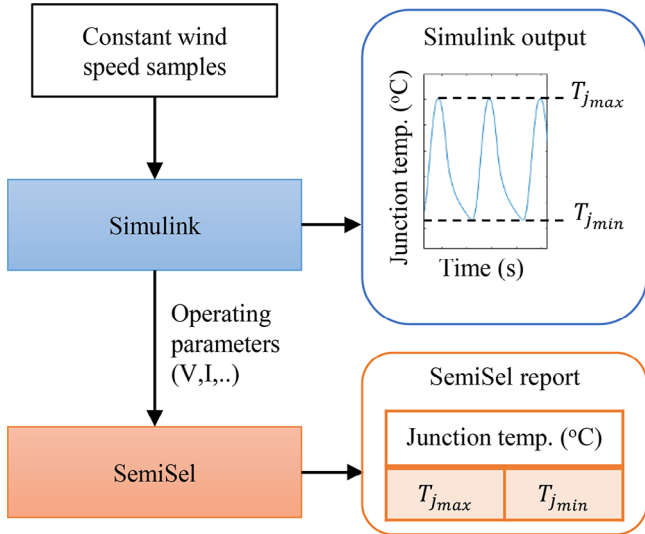


FIGURE 7 Simulation results validation procedure.

2.5 | Validation of simulation results

The precise result of semiconductor junction temperature is crucial for the WTPC lifetime estimation. Semiconductor lifetime is affected exponentially by the junction temperature mean (T_m) and range (ΔT) values as in Equation (5). The Simulink simulation model of the junction temperature is verified by comparing its results with the results of the manufacturer simulation tool, SemiSel [25]. SemiSel simulates the junction temperature of the converter semiconductors with fixed operating parameters (voltage, current, frequency, etc.). These fixed parameters can be extracted using constant wind speed simulation of the modelled WT. SemiSel's output report lists the minimum and maximum junction temperature, (T_{jmin}) and (T_{jmax}), which can be compared with the results of the Simulink model output. Simulink results comparison with SemiSel is used to determine the simulation accuracy. The procedure of the comparison between both results is shown in Figure 7. The results comparison is performed for nine constant wind speeds (4m/s, 5m/s,... 12m/s) which cover the WT's variable wind speed range. The results' accuracy is evaluated for each semiconductor by calculating the root mean square error (RMSE) of the results' relative differences (T_{jDif}) during all tested constant wind speeds. For each tested constant wind speed, T_{jDif} is calculated as in Equation (11) where T_{jSS} is the SemiSel simulation result and T_{jSL} is the Simulink simulation result. RMSE for each semiconductor is calculated as in Equation (12) for all the tested wind speeds where T_{jRSME} is the RMSE of the simulation results and k is the number of simulated constant wind speeds.

$$T_{jDif} = \frac{T_{jSS} - T_{jSL}}{T_{jSS}} \quad (11)$$

$$T_{jRSME} = \sqrt{\frac{\sum_{i=1}^k T_{jDif}^2}{k}} \quad (12)$$

TABLE 3 Junction temperature results RMSE.

Model	Semiconductor	$T_{jmax}(\%)$	$T_{jmin}(\%)$
2L-VSC	I1	0.24	0.18
	D1	0.43	0.19
3L-NPC	I1	0.15	0.15
	D1	0.94	0.93
	I2	0.83	0.26
	D2	0.81	1.4
	D5	2.1	0.83

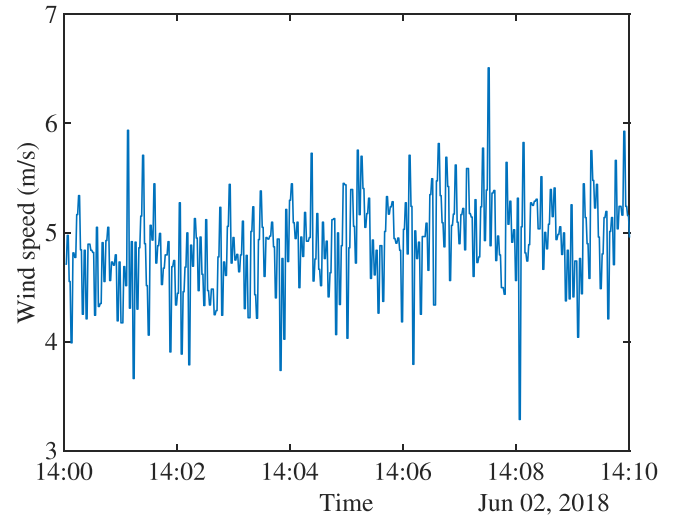


FIGURE 8 Example of 10 min WSTS.

The RMSE value is calculated for each semiconductor's T_{jmax} and T_{jmin} in both WTPC models. The calculated RMSE is shown in Table 3 where most of the values are less than 1 percent which indicates that the results of both WTPC models (2L-VSC and 3L-NPC) are accurate for the WTPC reliability analysis.

3 | EXPERIMENTAL RESULTS AND DISCUSSION

The WTPC reliability analysis is approached by applying a set of WSTS to the simulation model and analyzing the estimated lifetime against the wind properties, U_{avg} and TI. The WSTS are field-recorded wind speed data. Each WSTS is 10 min long and the wind speed is sampled at 1Hz, giving 600 wind speed measurements. The WSTS used in this paper are chosen from year-long wind speed data recorded by ORE Catapult in Blyth, UK. Figure 8 shows an example of one WSTS 4.89 m/s U_{avg} and 9 percent TI.

3.1 | Test 1: WTPC lifetime under WT operating wind speed

The effect of wind properties, U_{avg} and TI on the WTPC lifetime is analyzed in this test. The test includes simulating the

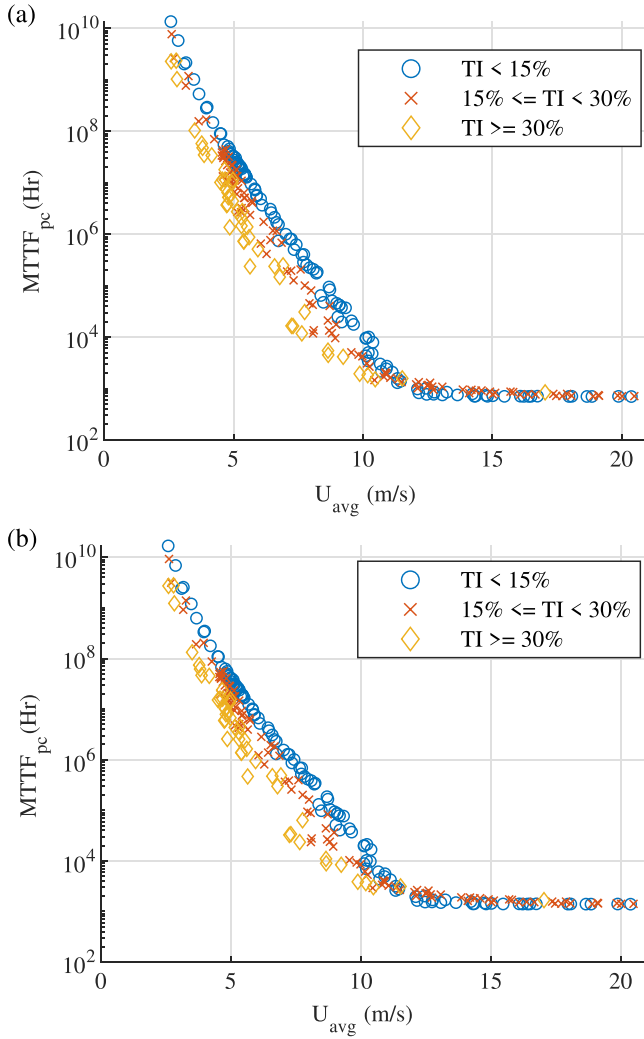


FIGURE 9 WTPC lifetime simulation results, (a) 2L-VSC and (b) 3L-NPC.

WTPC lifetime with a large number of WSTS to cover the WT operating range of wind speed and a wide range of TI. A set of 282 WSTS are selected for this test to cover U_{avg} range from 2.5 to 20.5 m/s and TI range of 1.81–42.36 percent. The simulation results for converter lifetime ($MTTF_{pc}$) are presented in a scatter diagram versus WSTS U_{avg} in Figure 9 for 2L-VSC and 3L-NPC models. To visualize the effect of the TI on the converter lifetime, the WSTS are grouped into three TI levels, less than 15 percent, between 15 and 30 percent, and above 30 percent. The TI groups are plotted in different colours and shapes in the scatter diagrams in Figure 9.

The WSTS U_{avg} shows a clear impact on the WTPC reliability in both WTPC topologies. As U_{avg} increases the MTTF decreases in a log scale until U_{avg} reaches the WT's rated wind speed where the MTTF does not reduce further because the WT pitch control is activated and reduces the blades' angle of attack to limit the WT power. On the other hand, The relationship between the WSTS TI and the WTPC lifetime can be seen in Figure 9 where the group of high TI WSTS (more than 30 percent) shows lower $MTTF_{pc}$ while the group of lower TI

TABLE 4 Mean and standard deviation of WTPC $\log(MTTF)$ for four TI groups of WSTS.

U_{avg} (m/s)	TI (%)	n	2L-VSC		3L-NPC	
			μ	σ	μ	σ
6	10	40	15.47	0.077	15.79	0.068
6	15	34	15.24	0.141	15.58	0.120
6	20	53	14.73	0.250	15.16	0.203
6	25	34	14.02	0.443	14.56	0.372

WSTS (less than 15 percent) shows higher $MTTF_{pc}$. However, the results overlap among the TI groups which appears because wind speed behaves differently in different WSTS even if they have the same average wind speed and the same TI. They therefore impact WTPC lifetime differently. Statistical methods will provide a better approach to analyze the impact of TI on the WTPC lifetime in the following test.

3.2 | Test 2: the impact of TI on WTPC lifetime

This test analyzes the impact of the TI on the WTPC lifetime. Since the wind TI includes complex patterns of wind speed variations, this test uses a statistical approach to evaluate the impact of TI on WTPC lifetime. For this, four sets of WSTS having the same average wind speed (6 m/s) but varying in their percentage TI (10, 15, 20, and 25) are applied to the simulation models. Each set includes a number of WSTS (n) simulated with WTPC models. The logarithmic values of the WTPC's lifetime ($\log(MTTF_{pc})$) are obtained for each tested WSTS. The statistical mean (μ) and standard deviation (σ) of each set results are calculated by Equations (13) and (14) respectively and shown in Table 4. The simulations' results of each set are applied to the statistical normality distribution test to clarify whether or not they are normally distributed. The Anderson–Darling test (AD test) [26] is selected as it is a widely used normality distribution test. The results of the four TI sets show that they are normally distributed so they can be represented by normal distribution fitting curves as shown in Figure 10 for the 2L-VSC and 3L-NPC.

This test proves that TI has impacted the WTPC lifetime. Although simulating individual WSTS may not show that clearly but the impact is clear when comparing the average WTPC lifetime of many WSTSs for different TI groups. This indicates that WTPC lifetime is impacted by the wind TI in the long run of the WT. Moreover, it can be observed that higher TI groups have a wider distribution curve (larger σ) than lower TI groups. This is because larger TI means higher variation in wind speed which is reflected in a wider distribution of WTPC lifetime estimates. This test examined the impact of TI related to one wind speed (6 m/s), while the next test analyzes the impact of the WTPC lifetime by TI for the range of WT operating wind speeds.

$$\mu = \frac{\sum_{i=1}^{i=n} \log(MTTF_{pc_i})}{n} \quad (13)$$

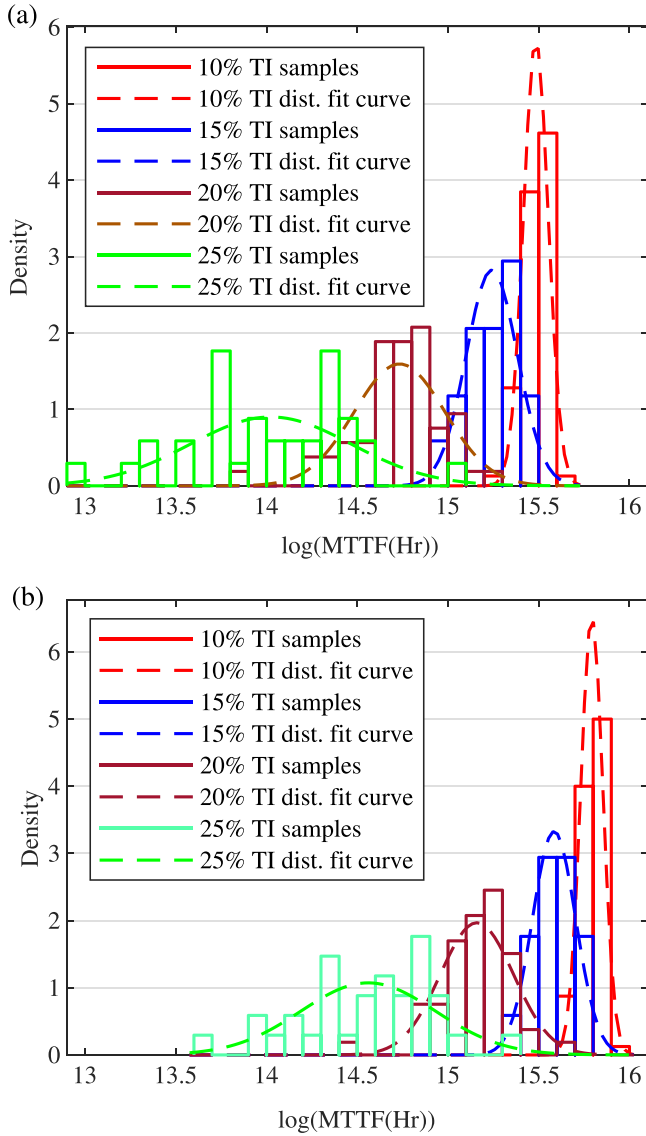


FIGURE 10 WTPC lifetime distributions of 10–25 percent TI WSTS with 6 m/s average wind speed, (a) 2L-VSC and (b) 3L-NPC.

$$\sigma = \sqrt{\frac{\sum_{i=1}^n \left(\log \left(\text{MTTF}_{\text{pc}_i} \right) - \mu \right)^2}{n}} \quad (14)$$

This test analyzes the impact of TI on the WTPC lifetime for a range of wind speeds to clarify the significance of TI impacts on the WTPC's lifetime. The test applies ten groups of WSTS on both WT models, 2L-VSC and 3L-NPC. The WSTS groups have U_{avg} of 4, 6, 8, 10, and 12 m/s, and TIs of 10 and 20 percent. The selected WSTS average wind speeds cover the WT variable speed range. The number of WSTS in each group (n) is shown in 5. For each group of WSTS, the average and standard deviation of logarithmic WTPC lifetimes are calculated by Equations (13) and (14) respectively. To analyze the statistical significance in lifetime differences between 10–20 percent TI for each U_{avg} , the confidence intervals (CI) are used. The CI is

TABLE 5 Lifetime comparison of two TI groups.

U_{avg} (m/s)	TI (%)	n	2L-VSC	3L-NPC
			CI	CI
4	10	34	19.33 ± 0.034	19.5 ± 0.036
6		40	15.47 ± 0.024	15.79 ± 0.021
8		35	12.21 ± 0.034	12.84 ± 0.029
10		35	9.09 ± 0.052	9.89 ± 0.054
12	20	35	6.95 ± 0.012	7.64 ± 0.012
4		35	18.83 ± 0.076	19.02 ± 0.072
6		53	14.73 ± 0.067	15.16 ± 0.045
8		35	11.18 ± 0.092	11.89 ± 0.091
10		34	8.17 ± 0.051	8.87 ± 0.051
12		35	7.16 ± 0.017	7.86 ± 0.017

calculated for a selected level of confidence where 95 percent is a widely accepted value in scientific research. The CI of the logarithmic lifetimes of each group is calculated by Equation (15) where α is the confidence level value which equals 1.96 for a 95 percent confidence level. The CI of the tested WSTS groups are shown in Table 5. The lifetime significance difference between the 10 and 20 percent groups can be illustrated using the error bars used to display CI as in Figure 11 for both 2L-VSC and 3L-NPC models. It is clearly shown that the results' CI do not overlap with most of the tested groups which are interpreted as lifetimes differences are significant between the two tested TIs. However, the WTPC lifetime of two TI groups overlapped near the rated wind speed and that is because the higher TI WSTS are more affected by the WT pitch control than the lower TI WSTS resulting in a more regulated rotating speed and therefore achieving higher WTPC lifetime values. This test proved that TI is significantly impacting the WTPC's lifetime for both 2L-VSC and 3L-NPC topologies.

$$\text{CI} = \mu \pm \alpha \frac{\sigma}{\sqrt{n}} \quad (15)$$

3.3 | Lifetime comparison between WTPC topologies

The previous reliability tests show that average wind speed and TI both affect WTPC lifetime for both tested topologies, 2L-VSC and 3L-NPC. Both topologies show similar impacts however the lifetime values (MTTF_{pc}) were different. The comparison between 2L-VSC and 3L-NPC lifetimes explores which one of them achieves a longer life at the tested conditions. The comparison is evaluated by calculating the lifetime ratio (LTR) of the 3L-NPC to the 2L-VSC as in Equation (16).

$$\text{LTR} = \frac{\text{MTTF}_{3\text{L-NPC}}}{\text{MTTF}_{2\text{L-VSC}}} \quad (16)$$

WTPC lifetime results are selected for LTR evaluation covering the WT operating wind speed range and belong to two

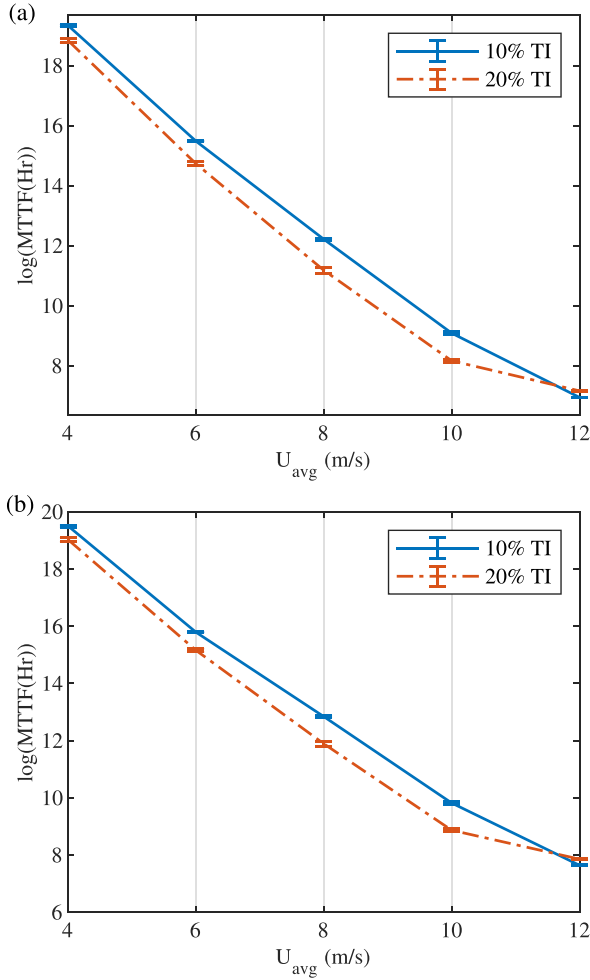


FIGURE 11 Lifetime of WTPC of 10 and 20 percent TI, (a) 2L-VSC and (b) 3L-NPC.

groups of TI (≤ 10 percent) and (≥ 25 percent) for clarity of the comparison. The WTPC lifetime results are presented in the scatter diagram in Figure 12 which clearly shows that LTR is affected by U_{avg} and TI. The results construct two trends for the two TI groups where both are increasing as the U_{avg} increase however the higher TI group (≥ 25 percent) shows higher LTR values than the ≤ 10 percent group for similar U_{avg} values. Therefore, it can confidently be concluded that the 3L-NPC WTPC can operate longer in time compared with 2L-VSC WTPC, especially with the high-speed and high-turbulence wind. The 3L-NPC topology shows a longer lifetime than 2L-VSC and that is because the converter load is distributed among more semiconductors in 3L-NPC. This results in lower temperature and therefore longer lifetime for 3L-NPC when compared with the 2L-VSC, particularly when subject to high turbulence intensities.

4 | CONCLUSIONS

This paper has examined the effects of average wind speed (U_{avg}) and turbulence intensity (TI) on the reliabilities of two

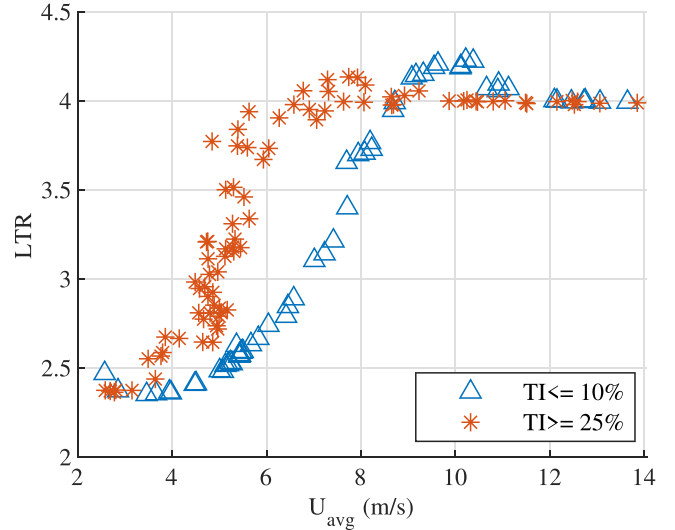


FIGURE 12 Lifetime comparison of 2L-VSC and 3L-NPC. LTR shows the lifetime ratio of 3L-NPC to 2L-VSC.

common WTPC topologies, 2L-VSC and 3L-NPC. The paper has applied statistical analysis to data from detailed electrical and thermal WTPC simulation and lifetime estimation to understand the effects of these two wind characteristics on WTPC lifetime. Lifetime was simulated for 821 10-min WSTS with wind speed sampled at 1Hz. The mean and standard deviation of the simulation results show clearly the relationship between wind conditions and WTPC lifetime. Furthermore, the results reveal how wind conditions interact differently according to the WTPC topology. The paper’s conclusions can be summarized as follows:

- Increased average wind speed has a direct and significant negative impact on the lifetime for both WTPC topologies, 2L-VSC and 3L-NPC.
- Higher wind TI causes lower WTPC lifetime in both converter topologies, 3L-NPC and 2L-VSC, however this impact is primarily noticeable over longer periods of WT operation.
- When comparing converter topologies for increasing average wind speed, the 3L-NPC converter achieves better reliability than the 2L-VSC. The 3L-NPC WTPC has an estimated lifetime 2.4 times that of the 2L-VSC WTPC at low average wind speed WSTS; this ratio increases as the WSTS average wind speed increases to reach 4.0 times the estimated lifetime at the WT rated wind speed.
- The 3L-NPC WTPC is more reliable than the 2L-VSC for higher TI wind.
- Wind turbulence and wind speed both have a noticeable effect on the reliability of the WTPC, and both should be considered for WTPC lifetime estimation and converter topology selection.

AUTHOR CONTRIBUTIONS

Sermed Alsaadi: Methodology; software; visualization; writing—original draft. **Christopher J. Crabtree:** Resources; supervision; writing—review and editing. **Peter C. Matthews:**

Supervision; writing—review and editing. **Mahmoud Shahbazi**: Supervision; writing—review and editing.

ACKNOWLEDGEMENTS

This paper is produced as part of the research funded by the UKRI EPSRC Prosperity Partnership in Offshore Wind EP/R0049/1. (npwg.group.shef.ac.uk).

CONFLICT OF INTEREST STATEMENT

The authors declare no conflicts of interest.

DATA AVAILABILITY STATEMENT

Data sharing not applicable - no new data generated

ORCID

Sermed Alsaadi  <https://orcid.org/0000-0002-1923-5358>

Christopher J. Crabtree  <https://orcid.org/0000-0003-0109-5323>

Mahmoud Shabbazi  <https://orcid.org/0000-0002-6057-3228>

REFERENCES

1. Dao, C., Kazemtabrizi, B., Crabtree, C.: Wind turbine reliability data review and impacts on levelised cost of energy. *Wind Energy* 22(12), 1848–1871 (2019)
2. Spinato, F., Tavner, P.J., Van Bussel, G.J.W., Koutoulakos, E.: Reliability of wind turbine subassemblies. *IET Renewable Power Gener.* 3(4), 387–401 (2009)
3. Fischer, K., Pelka, K., Bartschat, A., Tegmeier, B., Coronado, D., Broer, C., et al.: Reliability of power converters in wind turbines: Exploratory analysis of failure and operating data from a worldwide turbine fleet. *IEEE Trans. Power Electron.* 34(7), 6332–6344 (2019)
4. Blaabjerg, F., Liserre, M., Ma, K.: Power electronics converters for wind turbine systems. *IEEE Trans. Ind. Appl.* 48(2), 708–719 (2012)
5. Kovačević-Badstuebner, I.F., Kolar, J.W., Schilling, U.: Modelling for the lifetime prediction of power semiconductor modules. In: *Reliability of Power Electronic Converter Systems*, pp. 103–140. IET, London (2016)
6. Ye, S., Zhou, D., Yao, X., Blaabjerg, F.: Component-level reliability assessment of a direct-drive PMSG wind power converter considering two terms of thermal cycles and the parameter sensitivity analysis. *IEEE Trans. Power Electron.* 36(9), 10037–10050 (2021)
7. Isidoril, A., Rossi, F.M., Blaabjerg, F., Ma, K.: Thermal loading and reliability of 10-MW multilevel wind power converter at different wind roughness classes. *IEEE Trans. Ind. Appl.* 50(1), 484–494 (2014)
8. Busca, C., Teodorescu, R., Blaabjerg, F., Munk-Nielsen, S., Helle, L., Abeyasekera, T., et al.: An overview of the reliability prediction related aspects of high power IGBTs in wind power applications. *Microelectron. Reliab.* 51(9–11), 1903–1907 (2011)
9. Wintrich, A., Nicoai, U., Reimann, T., Tursky, W.: *Application Manual Power Semiconductors*. 2nd ed. ISLE Verlag, Ilmenau (2015)
10. Birk, J., Andresen, B.: Parallel-connected converters for optimizing efficiency, reliability and grid harmonics in a wind turbine. 2007 European Conference on Power Electronics and Applications, pp. 1–7. IEEE, Piscataway, NJ (2007)
11. Bayerer, R., Herrmann, T., Licht, T., Lutz, J., Feller, M.: Model for power cycling lifetime of IGBT modules – various factors influencing lifetime. In: *CIPS 2008-5th International Conference on Integrated Power Electronics Systems*, pp. 37–42. IEEE, Piscataway, NJ (2008)
12. GE. Haliade-X offshore wind turbine. <https://www.ge.com/renewableenergy/wind-energy/offshore-wind/haliade-x-offshore-turbine> (2021). Accessed 8 June 2023
13. Samsung Heavy industries. Samsung Wind Energy Solutions (2015). <http://www.samsungshi.com/eng/default.aspx>. Accessed 4 June 2020
14. Smith, C.J., Crabtree, C.J., Matthews, P.C.: Impact of wind conditions on thermal loading of PMSG wind turbine power converters. *IET Power Electron.* 10(11), 1268–1278 (2017)
15. Kostandyan, E.E., Ma, K.: Reliability estimation with uncertainties consideration for high power IGBTs in 2.3 MW wind turbine converter system. *Microelectron. Reliab.* 52, 2403–2408 (2012)
16. Anderson, P.M., Bose, A.: Stability simulation of wind turbine systems. *IEEE Power Eng. Rev.* 3(12), 32–32 (1983)
17. Li, H., Ji, H., Li, Y., Liu, S., Yang, D., Qin, X., et al.: Reliability evaluation model of wind power converter system considering variable wind profiles. In: *2014 IEEE Energy Conversion Congress and Exposition, ECCE 2014*, pp. 3051–3058. IEEE, Piscataway, NJ (2014)
18. Baygildina, E., Peltoniemi, P., Pyrhonen, O., Ma, K., Blaabjerg, F.: Thermal loading of wind power converter considering dynamics of wind speed. In: *IECON Proceedings Industrial Electronics Conference*, pp. 1362–1367. IEEE, Piscataway, NJ (2013)
19. Wu, B., Lang, Y., Zargari, N., Kouro, S.: *Power Conversion and Control of Wind Energy System*. vol. 148, Wiley, New York (2011)
20. Fischer, K., Stalin, T., Ramberg, H., Wenske, J., Wetter, G., Karlsson, R., et al.: Field-experience based root-cause analysis of power-converter failure in wind turbines. *IEEE Trans. Power Electron.* 30(5), 2481–2492 (2015)
21. SEMIKRON DANFOSS. SKM800GA176D IGBT Module. <https://www.semikron-danfoss.com/products/product-classes/igbt-modules/detail/skm800ga176d-22890435.html>. Accessed 12 June 2023
22. Andresen, B., Birk, J.: A high power density converter system for the Gamesa G10x 4,5 MW wind turbine. In: *2007 European Conference on Power Electronics and Applications, EPE*, pp. 1–8. IEEE, Piscataway, NJ (2007)
23. The Mathworks Inc. Semscape 5.0. <https://www.mathworks.com/products/simscape.html>. Accessed 22 September 2022
24. Miner, M.A.: Cumulative damage in fatigue. *J. Appl. Mech., Trans.* 12(3), A159–A164 (1945)
25. SEMIKRON INTERNATIONAL GmbH. SemiSel. <https://semisel.semikron.com> (2021). Accessed 9 Feb 2022
26. Anderson, T.W., Darling, D.A.: A Test of Goodness of Fit. *J. Am. Stat. Assoc.* 49(268), 765–769 (1954). <https://www.tandfonline.com/doi/abs/10.1080/01621459.1954.10501232>

How to cite this article: Alsaadi, S., Crabtree, C.J., Matthews, P.C., Shahbazi, M.: Understanding wind turbine power converter reliability under realistic wind conditions. *IET Power Electron.* 1–10 (2024). <https://doi.org/10.1049/pel2.12670>